Steerable Mechanical Joint for High Load Transmission in Minimally Invasive Instruments

Tin Yan Nai
e-mail: timnai@gmail.com

Just L. Herder
e-mail: j.l.herder@tudelft.nl

Department of Biomechanical Engineering,
Faculty of Mechanical, Maritime and Materials Engineering,
Delft University of Technology,
Delft, The Netherlands

Gabriëlle J. M. Tuijthof[1]
Department of Biomechanical Engineering,
Faculty of Mechanical, Maritime and Materials Engineering,
Delft University of Technology,
Delft, The Netherlands;
Orthopedic Research Center Amsterdam,
Department of Orthopedic Surgery,
Academic Medical Centre,
Amsterdam, The Netherlands
e-mail: g.j.m.tuijthof@tudelft.nl; g.j.tuijthof@amc.uva.nl

As minimally invasive operations are performed through small portals, the limited manipulation capability of straight surgical instruments is an issue. Access to the pathology site can be challenging, especially in confined anatomic areas with few available portals, such as the knee joint. The goal in this paper is to present and evaluate a new sideways-steerable instrument joint that fits within a small diameter and enables transmission of relative high forces (e.g., for cutting of tough tissue). Meniscectomy was selected as a target procedure for which quantitative design criteria were formulated. The steering mechanism consists of a crossed configuration of a compliant rolling-contact element that forms the instrument joint, which is rotated by flexural steering beams that are configured in a parallelogram mechanism. The actuation of cutting is performed by steel wire that runs through the center of rotation of the instrument joint. A prototype of the concept was fabricated and evaluated technically. The prototype demonstrated a range of motion between −22° and 25° with a steering stiffness of 17.6 Nmm/rad (min 16.9 – max 18.2 Nmm/rad). Mechanical tests confirmed that the prototype can transmit an axial load of 200 N on the tip with a maximum parasitic deflection of 4.4°. A new sideways steerable mechanical instrument joint was designed to improve sideways range of motion while enabling the cutting of strong tissues in a minimally invasive procedure. Proof of principle was achieved for the main criteria, which encourages the future development of a complete instrument. [DOI: 10.1115/1.4004649]

Keywords: compliant mechanism, meniscectomy, steerable mechanical joint, rolling contact

1 Introduction

As minimally invasive operations are performed through small portals and the manipulation capability of straight surgical instruments is limited, access to the pathology site can be challenging [1]. This is especially true for body cavities with confined spaces and few available access portals [2]. An example is the human knee joint, which is surrounded by bones, ligaments, and neurovascular structures [3].

To increase the manoeuvrability of minimally invasive surgical instruments, different concepts of steerable mechanisms have been presented to enhance instrument manipulation capability (e.g., Refs. [1,4–8]). Often the focus is on achieving maximum range of motion, multiple degrees of freedom, or miniaturisation, which is well suited for the intended application. However, it is doubtful whether applying these concepts is feasible for manipulating or cutting of tough tissue, such as a torn meniscus located in the knee joint [9].

Therefore, the goal is to present and to evaluate a sideways steerable mechanical joint that fits within a small diameter *and* is able to withstand relatively high force transmission.

2 Design Requirements

Formulation of quantitative design requirements was performed by choosing one minimally invasive procedure for which application would be beneficial: meniscectomy. Meniscectomy is performed around 1.7×10^6 times a year worldwide [10] and consists of surgical removal of a meniscal lesion to create a stable rim [11]. Design requirements are summarized in Table 1. The maximum cutting force (F_c) was calculated to be approximately 190 N, using the maximum shear stress for punching meniscal tissue (10.2 N/mm^2) [12] and the circumferential cutting area of a conventional cutter (19 mm^2). F_c acts as compressive force on the proposed steerable mechanical joint. The required range of motion (RM_{tip}) was estimated to be −55° to 55° relative to the instrument shaft in the meniscal plane [2]. For comfortable steering, a low steering stiffness (K) is preferred. The main geometric criteria are a maximum outer shaft diameter (d_{shaft}) to fit the access portal, and a minimum shaft length (L_{shaft}) to easily feed the whole instrument in the knee joint [2] (Table 1).

To guarantee robust function when handling the instrument, two critical situations can be identified. First, during insertion of the instrument in an access portal, the tip should remain in line with the shaft to minimize the risk of damaging healthy tissue. This requires minimal deflection of the tip under axial ($F_{exaxial}$) and transverse ($F_{extrans}$) loads (Table 1). Secondly, during tissue cutting a maximum parasitic deflection (φ_p) of 5° is allowed [2].

3 Conceptual Design

The steerable mechanical instrument joint function was divided into *steering* and *cutting*, with steering split into *hinging* of mechanical parts and *actuating* them.

Traditional mechanisms using gears, pulleys, or linkages [1,13] and actuation by hydraulics [14] or pneumatics pose a challenge for the intended design, because possibilities for miniaturization are limited. Compliant mechanisms in which the deflection of designated flexible members transmits force, motion, and energy [15], do not have these drawbacks. As a result, fewer parts are required, leaving more construction space, reduced backlash, and wear. However, application of compliant mechanisms for surgical instruments was primarily performed for grasping soft tissues [8,16–19], and design synthesis when dealing with large deflections, interconnected deformations, and three-dimensional structures pose problems [19].

To avoid complex three-dimensional structures, the cutting mechanism was placed distally at the instrument tip and the steering mechanism proximally behind the cutting mechanism. This strategy allows superposition of two-dimensional solutions to achieve synthesis.

Many compliant hinges only allow small displacements to remain within the elastic deformation zone and to prevent buckling

[1]Corresponding author.

Manuscript received December 16, 2010; final manuscript received June 21, 2011; published online September 30, 2011. Assoc. Editor: Vijay Goel.

Table 1 Design requirements [2] and experimental results of the steerable mechanical joint using meniscectomy as an example for application

Parameter	Symbol	Requirement	Experimental result
Cutting force	F_c	$\geq$ 190 N	Transmission of 200 N
Shaft diameter	d_{shaft}	$\geq$ 5 mm	5 mm
Tip length	L_{tip}	$\geq$ 15 mm	Conventional tip
Shaft length	L_{shaft}	$\leq$ 105 mm	125 mm
Range of motion of tip	RM_{tip}	$-55°$ to $55°$	$-22°$ to $25°$
Sideways steering stiffness of mechanical joint	K	Low	17.6 Nmm/rad (min 16.9 – max 18.2 Nmm/rad)
External axial load at tip	F_{exaxial}	$\leq$ 5 N	Transmission of 200 N
External transverse load at tip	F_{extrans}	$\leq$ 10 N	$K_{\text{locked}} = 639$ Nmm/rad[a]
Parasitic deflection at 200 N	φ_p	$\geq 5°$	$4.1°$ (min $3.6°$ – max $4.4°$)

[a]Application of 10 N of transverse load at the tip at a distance L_{tip} of 15 mm results in $13°$ of parasitic deflection.

(e.g., Refs. [8,15–17,20]). A compliant rolling-contact element (CORE) appeared to be suitable for our purpose [21,22]. A CORE is a rolling contact mechanical joint in which two rounded solid parts are connected by a compliant crossed flexure, which prevents relative sliding motion of the solid parts (Fig. 1(*b*)). As a result, the contact surfaces of each of the solid parts can roll relative to each other without slip and transmit high axial loads.

Typical compliant solutions for steering consisted of tape springs [23], contact aided mechanisms [24], a compliant Chebyshev linkage [12], and compliant crank sliders [15]. Initial calculations showed that a combination of two tape springs named flexural steering beams (FSBs) and a compliant parallelogram mechanism [25] gave a promising solution (Fig. 1(*a*)). This embodiment consisted of a rigid rectangular shaft with two identical CORE joints on each end. The COREs are connected by two FSBs located along each side of the shaft. The FSBs are guided in a round tube to allow bending only at the level of both COREs (Fig. 1(*b*)) and to form a compliant parallelogram mechanism. Rotation of one CORE end (the handle part) causes the opposite CORE end (instrument tip) to rotate equally (Fig. 1).

Actuation of the cutting mechanism was kept simple by two steel wires that allow opening and closing the instrument jaw (Fig. 1). A critical design feature is that the steel wires need to be guided through the centers of the pivot points to prevent undesired moments on the steerable mechanical joint.

4 Dimensional Design

To start the dimensioning process, constraints were set:

- d_{shaft} was set at 5 mm, with an inner radius r_{in} of 2 mm (Fig. 1, Table 2).
- Stainless steel type_301_CR was used in the calculations (material properties see Table II) [15]
- CORE joint is fabricated out of plate material

4.1 Compliant Rolling-Contact Element (CORE). Several dimensions are crucial for the CORE: w_{core}, h_{core}, r_{core}, and t_{core} (Fig. 1(*b*) and 1(*c*)).

As the CORE is fabricated out of plate material, its cross section has to be rectangular and fit within a diameter of 4 mm (Fig. 1(*c*)). RM_{tip} can be achieved with the chosen values for w_{core}, h_{core}, and r_{core} (Table II).

To calculate t_{core} the following assumptions were made:

- The crossed flexure material is linearly elastic, isotropic and homogeneous
- The bending component of the deflection is dominant

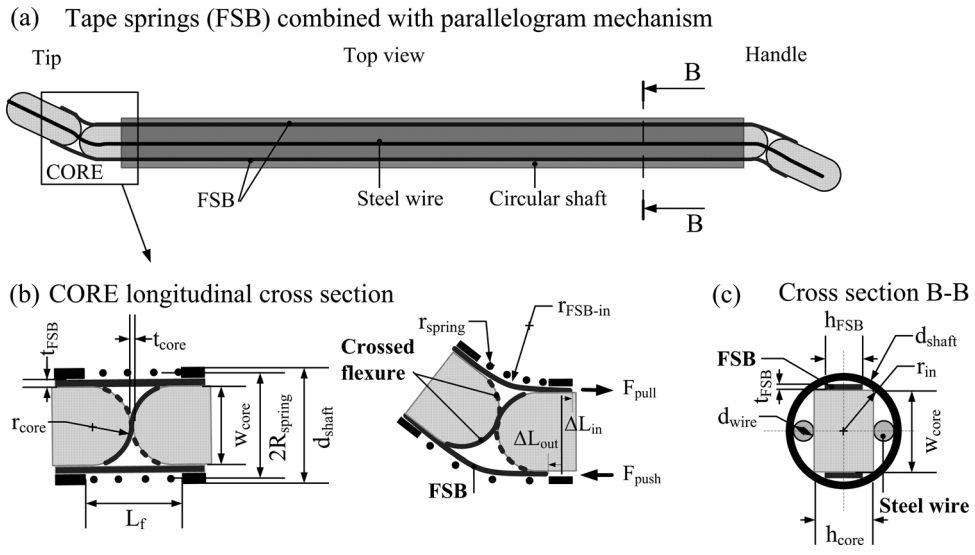

Fig. 1 (*a*) The circular shaft (transparent) with handle and instrument tip demonstrates the concept of the sideways steerable instrument using a parallelogram configuration and two tape springs (flexural steering beams (FSBs)). (*b*) Cross section of one compliant rolling element (CORE) that is flanked by two FSBs and is surrounded by a spring (the steel wire is omitted). (*c*) Cross section B-B is the transverse cross section of the shaft showing a stacked pair of monolithic layers in the center which are flanked by the two FSBs, and the steel wires; and surrounded by the circular shaft. All relevant dimensions are indicated (values are available in Table II).

Table 2 Parameters, symbols, and values, which were initially chosen or calculated. The last column presents the values used in the prototype.

Parameter	Symbol	Value chosen for calculations	Value in prototype
CORE width	w_{core}	3 mm	3 mm
CORE height	h_{core}	2 mm	2 mm
CORE contact radius	r_{core}	3 mm	3 mm
FSB inner radius at 55° of bending	$r_{FSB\text{-}in}$	6 mm	6 mm
unguided part of FSB length	L_f	8 mm	8 mm
FSB height	h_{FSB}	2 mm	2 mm
Yield strength stainless steel	$\sigma_{bending}$	1138 MPa	
Stainless steel modulus of elasticity	E	197 GPa	
Stainless steel Poisson coefficient	ν	0.29	
Helical spring number of active coils	n	10	10
Helical spring wire radius	r_{spring}	0.15 mm	0.15 mm
Helical spring radius	R_{spring}	2.2 mm	2.2 mm
Steel wire diameter	d_{wire}	0.4 mm	0.4 mm
		Value calculated	Value in prototype
CORE thickness of the cross flexure	t_{core}	$\leq$ 0.034 mm	0.028 mm
FSB thickness	t_{FSB}	$\leq$ 0.07 mm	0.069 mm

- The neutral axis of the crossed flexure coincides with the geometric centroid axis

In the neutral straight position of the CORE, the curved crossed flexures are unstressed (Fig. 1(*b*)). When the cutting force (F_c) has to be transmitted, the two rounded contact surfaces of the CORE (r_{core}) are compressed. The Hertz line contact stresses in the crossed flexures should remain within the elastic region of deformation [26]. The bending stress can be calculated with the Bernoulli–Euler equation [27]:

$$\sigma_{bending} = \frac{Et}{2R} \tag{1}$$

where t is the thickness of the thin beam and R is the radius of the constraining circular surface.

When $\sigma_{bending}$, E and the maximum value for r_{core} are substituted in Eq. (1), the maximum t_{core} is calculated to be 0.034 mm.

4.2 Flexural Steering Beam (FSB). To calculate t_{FSB}, Eq. (1) is used while assuming pure bending of the FSBs around a circular curvature of $r_{FSB\text{-}in}$ (Fig. 1(*b*), Table 2). At 55°, a maximum t_{FSB} of 0.07 mm is calculated.

4.3 Steering Stiffness. The sideways steering stiffness (K) of the COREs when actuating the FSBs was calculated to determine reasonable actuation forces. The entire instrument has two sideways steerable mechanical joints (Fig. 1(*a*)), each consisting of one CORE, two FSBs and one helical compression spring (Fig. 1(*b*)). Thus, K is calculated by the summation of these parallel positioned spring-elements:

$$K = 2K_{f-core} + 4K_{FSB} + 2K_{OC}. \tag{2}$$

The bending stiffness of each crossed flexure in the CORE ($K_{f\text{-}core}$) and each deflection zone of the FSBs (K_{FSB}) are approximated using linear beam theory [15]:

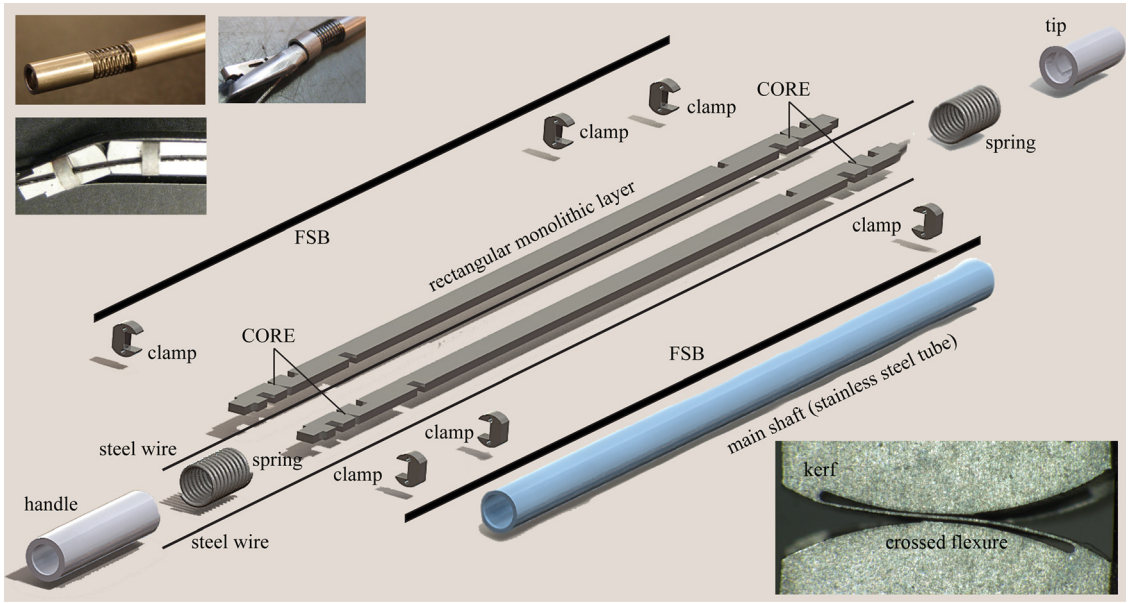

Fig. 2 Exploded view of all parts of the prototype. Photographs top left: Fully assembled prototype where two steel tubes fixate a spring mounted around a CORE. Two assembled monolithic layers zoomed in at one CORE, where two FSBs are welded to the sides and the steel wire runs through the holes in the clamps. An existing instrument tip mounted on the prototype for demonstration. Photograph bottom right: Magnified photograph of two stacked COREs with crossed flexures t_{core} of 0.028 mm.

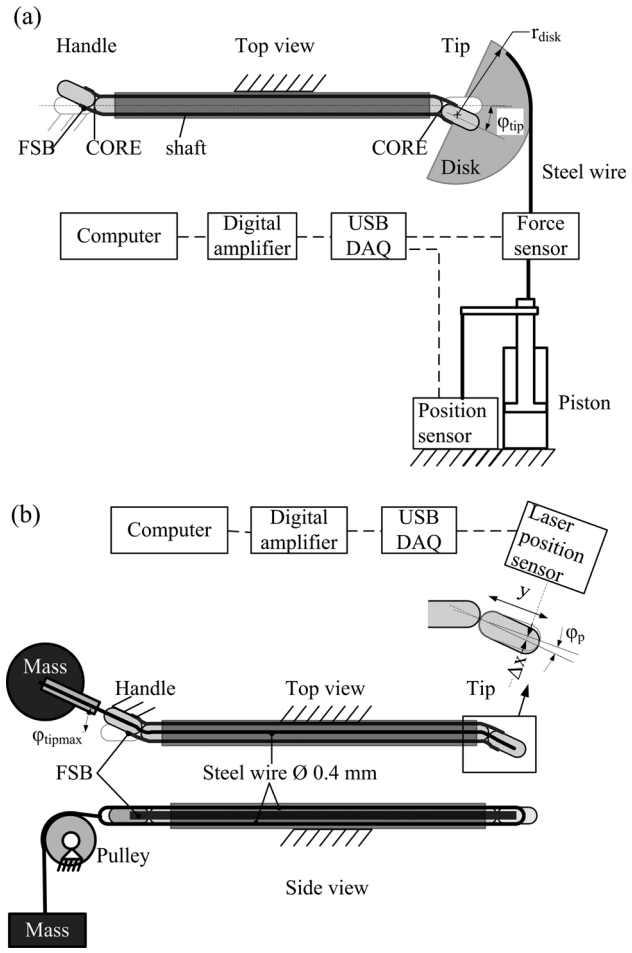

Fig. 3 Experimental set up in two configurations. (*a*) Set up to measure RM_{tip}, K, and K_{locked}. The instrument tip is fixed within in the semicircular disk. The steel cable is attached to the outer surface of the disk and to the force sensor. A piston pulls the steel cable. Simultaneously displacement is measured with the magnetostrictive position sensor. (*b*) Set up to measure φ_p. The mass runs along a pulley and is connected to the steel wire, which runs superiorly through the prototype and runs back inferiorly. The prototype is clamped in its greatest steering angle φ_{tipmax}. The displacement between unloaded and loaded instrument tip is measured with a laser displacement sensor (see enlarged drawing where φ_p is indicated).

$$K = \frac{EI}{L} \tag{3}$$

To calculate $K_{f\text{-core}}$, substitute $L = 0.25\text{RM}_{tip}(\pi/180)r_{core}$ and $I = h_{core}t_{core}^3/12$ in Eq. (3) and use the values in Table 2: 0.9 N mm/rad. To calculate K_{FSB} representing one FSB, substitute $L = L_f$ and $I = h_{FSB}t_{FSB}^3/12$ in Eq. (3) and use the values in Table 2: 1.4 Nmm/rad. The bending stiffness of an open coiled helical spring (K_{OC}) is calculated with the estimation from Lotti *et al.* [28]:

$$K_{OC} \approx \frac{E}{4(2+\nu)n}\frac{r_{spring}^4}{R_{spring}} \tag{4}$$

where n is the number of active coils, r_{spring} is the wire radius, and the R_{spring} is the mean helix radius (Fig. 1(*b*)). Using the values of Table 2, K_{OC} is approximately 0.5 N mm/rad.

K is estimated to be 8.4 N mm/rad using Eq. (2). This implies that, with a moment arm of 15 mm, around 0.5 N of actuating force has to be generated to rotate the instrument tip 55°.

5 Prototype

For ease of manufacturing and assembly, some parts were integrated in a single compliant piece. Using the symmetry of the COREs and the suggestion from Ref. [27], two identical monolithic layers were laser milled from stainless steel_301_CR and stacked in a mirrored fashion to form the inner rectangular shaft (Fig. 2). Both ends contain one CORE representing the instrument tip and the handle (Figs. 1,2). The crossed flexures have a wall thickness of 0.028 mm (Fig. 2). Six circular shaped clamps are placed along the stacked monolithic layers to keep them together. Two holes (Ø 0.6 mm) in each clamp guide the steel wires (d_{wire} is 0.4 mm) for actuation of the cutting mechanism. The prototype allows only closing of the jaw. The two FSBs are made of stainless steel foil (0.069 mm) and micro welded. A stainless steel tube (Ø 5×4 mm) functions as outer shaft that provides structural rigidity. Two steel tubes are mounted on each end to fixate the two springs at the level of the COREs, and to house the clamps and the FSBs. For demonstrative purposes, the cutter from a conventional arthroscopic punch was fitted on the tip (Fig. 2).

6 Experimental Evaluation

Measurements were performed to determine four parameters: the range of motion of the tip (RM_{tip}), the steering stiffness (K), the resistance against an external transverse load at the tip defined as the bending stiffness of the locked sideways steerable instrument (K_{locked}), and the parasitic deflection at 20 kg (φ_p) (Table I).

The RM_{tip} and K were measured in one experiment where a moment was applied on the tip of the instrument and its angular deflection was measured. K is the slope of the deflection-moment relation. K_{locked} is measured in the same setup with φ_{tip} is equal to zero degrees, which is the most critical position for sideways loading. To keep this straight position, the handle end was locked in line with the shaft (Fig. 3(*a*)). Subsequently, a sideways moment was applied at the tip by a force that was generated by a piston and transmitted to a preloaded cable that was attached to a semicircular disk ($r_{disk} = 20.31$ mm) (Fig. 3(*a*)). The piston induced displacement was measured with a magnetostrictive position sensor (LCIT 2000, Feteris Components Benelux, Den Haag, The Netherlands), and the resulting force with a 500N force sensor (H3G-C3-50kg-6B, Zemic, Etten-Leur, The Netherlands). Both signals were fed through a data acquisition module (USB-6008, National Instruments, Austin, USA) and led to an amplifier (CPJ2sRail, SCAIME, Annemasse cedex, France) (Fig. 3(*a*)). Custom written software in LABVIEW 8.2.1(National Instrument, Austin, USA) was used to log all data at 1 kHz. Each measurement was performed in a quasistatic manner, where the load was increased stepwise with pauses of a couple of seconds. Both conditions K and K_{locked} were repeated four times. All data processing was performed with MATLAB R2009a (The MathWorks, Inc, Natick, USA). The presence of a linear relation between the mean value of the moments and the corresponding mean value of φ_{tip} was determined from which the slopes K and K_{locked} were calculated.

Critical parasitic angular deflection (φ_p) occurs at maximum φ_{tip} when the instrument is cutting tissue. This situation was simulated in the prototype by axial loading of the mechanical joint. The main shaft was secured and the handle end was locked at maximum φ_{tip} (20°) (Fig. 3(*b*)). A steel wire was looped from the handle around the tip and back. Both ends of the wire were clipped together and connected to masses (increasing from 5, 10, 15, to 20 kg), that caused axial loading on the mechanical joint (Fig. 3(*b*)). When loaded with a mass, the displacement of the instrument tip was measured with a laser displacement sensor (optoNCDT IDL1401-10, Micro-Epsilon, Ortenburg, Germany). Measurements were repeated four times. For data processing, the travel of the pivot point of the CORE joint was neglected. φ_p was determined by measuring the change in tip displacement and the distance between the laser point on the tip and the pivot point

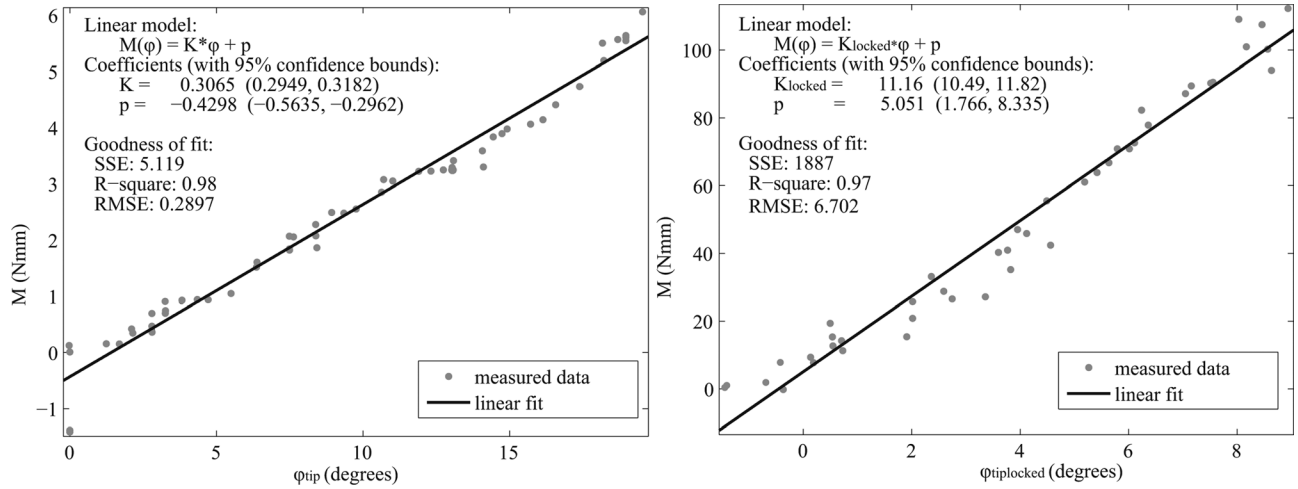

Fig. 4 Results of the moment- angular deflection measurements from which *K* and K_{locked} where determined. Angular deflection of the instrument tip caused by an applied moment in (*a*) a free mode and (*b*) a locked mode.

followed by application of the tangent rule. The maximum φ_p was calculated as the mean value for loading with 20 kg.

7 Results

Table I shows a summary of the results of the experiments in the last column. RM_{tip} was measured to fall between +25° and −22°. A linear relation was found between φ_{tip} and applied moments (Fig. 4) resulting in a mean $K = 17.6$ N mm/rad (min 16.9 – max 18.2 N mm/rad), and a resistance against external transverse loads expressed by a mean $K_{locked} = 639$ N mm/rad (min 601 – max 677 N mm/rad). The parasitic deflection φ_p was between 3.6° and 4.4° for an axial load of 20 kg.

8 Discussion

The goal was to design a sideways steerable mechanical joint, which can provide a relatively large range of motion (50°) that fits within a small diameter (Ø 5 mm) and can sustain relatively high axial loading (up to 200 N). This was achieved by a robust supporting base embodied with compliant elements that form the hinge (CORE) and the steering mechanism (compliant parallelogram linkage FSB). Initial calculations demonstrated that the design should meet the requirements. This was largely confirmed by evaluation of a prototype (Table 1).

The steerable mechanical joint was able to resist an external axial load of 20 kg without breaking and with a maximum parasitic angular deflection of 4.4°. If the ratio of the moment arms of the cable and the center of the cutting load are assumed to be equal, F_c can be generated. A redesign of the instrument beak to lower F_c could complement the design.

Unfortunately, RM_{tip} was met for 50% (Table 1) and a difference in the two maxima was present. Several factors could have contributed: (a) difference between material properties used for calculation and actual values, (b) assembly tolerances, and (c) the improper positioning of the kerf in the cross flexures at each end (Fig. 2), which functionally served as a mechanical stop and prevented further rotation. The former two could also explain the difference between the calculated and the measured value of *K* (Table I).

Robust function against external loading also depends on the method of application. For meniscectomy, external axial loading of 5 N was met. However, external transversal loading of 4 N caused an angular parasitic deflection of 5°. This latter is probably not acceptable for meniscectomy, as a previous study indicated that adequate resistance against external loading is crucial to give a good sense of control [2,29].

The relatively low number of components and the ease of assembly suggest that this design is probably more attractive in a disposable or semidisposable configuration. Additionally, this would avoid the breaking of parts due to high repetitive loading.

Comparing the new steerable mechanical joint with four other steerable mechanisms, which presented similar technical data [4–7], indicates that those generally offer a wider range of motion at the cost of less resistance against loading.

9 Conclusion

An innovative compliant steerable mechanical joint was developed that fits within Ø 5 mm, has a range of motion of 50° and is capable to withstand axial loading of 200 N. This concept can be used as a building block for future designs of minimally invasive surgical instruments.

References

[1] Lim, J., and Erdman, A., 2003, "A Review of Mechanism Used in Laparoscopic Surgical Instruments," Mech. Mach. Theory, **38**, pp. 1133–1147.

[2] Tuijthof, G. J. M., 2003, "Technical Improvement of Arthroscopic Techniques," Ph.D. thesis, Delft University of Technology, Delft, The Netherlands.

[3] Arnoczky, S. P., 1990, "Structure and Biology of the Knee Meniscus," in *Biomechanics of Diarthrodial Joints*, V. C. Mow, A. Ratcliffe, and S. L.-Y. Woo, eds., Springer-Verlag, New York, Chap. 6, pp. 177–190.

[4] Frecker, M. I., and Snyder, A. J., 2005, "Surgical Robotics: Multifunctional End Effectors for Robotic Surgery," Oper. Tech. General Surgery, **7**(4), pp. 165–169.

[5] Hasuo, T., Ogura, G., Sakuma, I., Kobayashi, E., Iseki, H., and Nakamura, R., 2006, "Development of Bending and Grasping Manipulator for Multi Degrees of Freedom Ultrasonically Activated Scalpel," Int. J. Comput. Assisted Radiol. Surgery, **1**(suppl. 7), pp. 222–223.

[6] Yamashita, H., Kim, D., Hata, N., and Dohi, T., 2003, "Multi-Slider Linkage Mechanism for Endoscopic Forceps Manipulator," in *Conference on Intelligent Robots and Systems*, pp. 2577–2582.

[7] van Meer, F., Philippi, J., Esteve, D., and Dombre, E., 2007, "Compact Generic Multi Channel Plastic Joint for Surgical Instrumentation," Mechatronics, **17**, pp. 562–56.

[8] Balazs, M., Feussner, H., Hirzinger, G., Omote, K., and Ungeheuer, A., 1998, "A New Tool for Minor-Access Surgery," IEEE Eng. Med. Biol., **May/June**, pp. 45–48.

[9] Kelly, M. A., Fithian, D. C., Chern, K. Y., and Mow V. C., 1990, "Structure and Function of the Meniscus: Basic and Clinical Implications," in *Biomechanics of Diarthrodial Joints*, V. C. Mow, A. Ratcliffe, and S. L.-Y. Woo, eds., Springer-Verlag, New York.

[10] Baker, B., and Lubowitz, J., "Meniscus Injuries," eMedicine, updated 22 November 2006, accessed 24 August 2007, available from http://www.emedicine.com/sports/topic160.htm

[11] Howell, J. R., and Handoll, H. H., 2000, "Surgical Treatment for Meniscal Injuries of the Knee in Adults," Cochrane. Database. Syst. Rev., **2**, pp. CD001353.

[12] Tuijthof, G., Meulman, H., Herder, J., and Dijk, C. v., 2009, "Meniscal Shear Stress for Punching," J. Appl. Biomater. Biomech., **7**(2), pp. 97–103.
[13] Sclater, N., and Chironis, N., 2007, *Mechanisms and Mechanical Devices*, McGraw-Hill, New York.
[14] Ikuta, K., Ichikawa, H., Suzuki, K., and Yamamoto, T., 2003, "Safety Active Catheter With Multi-Segments Driven by Innovative Hydro-Pressure Micro Actuators," in *16th Annual International Conference on IEEE Micro Electro Mechanical Systems (MEMS)*, pp. 130–135.
[15] Howell, L., 2001, *Compliant Mechanisms*, Wiley, New York.
[16] Frecker, M. I., Powell, K. M., and Haluck, R., 2005, "Design of a Multifunctional Compliant Instrument for Minimally Invasive Surgery," J. Biomech. Eng, **127**(6), pp. 990–993.
[17] Herder, J., and van den Berg, F., 2000, "Statically Balanced Compliant Mechanisms (SBCM'S), and Example and Prospects," *ASME 2000 International Design Engineering Technical Conferences and Computers and Information in Engineering Conference*, Baltimore, Paper No. DETC2000/MECH-14144.
[18] de Lange, D., Langelaar, M., and Herder, J., 2008, "Towards the Design of a Statically Balanced Compliant Laparoscopic Grasper Using Topology Optimization," *ASME 2008 International Design Engineering Technical Conferences and Computers and Information in Engineering Conference*, Paper No. DETC2008-49794, pp. 293–305.
[19] Kota, S., Lu, K. J., Kreiner, K., Trease, B., Arenas, J., and Geiger, J., 2005, "Design and Application of Compliant Mechanisms for Surgical Tools," J. Biomech. Eng, **127**(6), pp. 981–989.
[20] Trease, B., Moon, Y.-M., and Kota, S., 2005, "Design of Large-Displacement Compliant Joints," J. Mech. Des., **127**, pp. 788–798.
[21] Jeanneau, A., Herder, J., Laliberte, T., and Gosselin, C., 2004, "A Compliant Rolling Contact Joint and its Application in a 3-DOF Planar Parallel Mechanism With Kinematic Analysis," in *Proceedings of the ASME Design Engineering Technical Conference*, Salt Lake City, pp. 689–698.
[22] Halverson, P., Howell, L., and Magleby, S., 2010, "Tension-Based Multi-Stable Compliant Rolling-Contact Elements," Mech. Mach. Theory, **45**(2), pp. 147–156.
[23] Soykasap, O., 2007, "Analysis of Tape Spring Hinges," Int. J. Mech. Sci., **49**(7), pp. 853–860.
[24] Yamashita, H., Matsumiya, K., Masamune, K., Liao, H., Chiba, T., and Dohi, T., 2006, "Two-DOFs Bending Forceps Manipulator of 3.5-mm Diameter for Intrauterine Fetus Surgery: Feasibility Evaluation," Int. J. Comput. Assisted Radiol. Surgery, **1**(suppl 1), pp. 218–220.
[25] Breedveld, P., Scheltes, J., Blom, E., and Verheij, J., 2005, "A New, Easily Miniaturized Steerable Endoscope," IEEE Eng. Med. Biol. Mag., pp. 40–47.
[26] van Beek, A., 2006, Advanced Engineering Design: Lifetime Performance and Reliability, Technische Universiteit Delft, Delft.
[27] Cannon, J., Lusk, C., and Howell, L., 2005, "Compliant Rolling-Contact Element Mechanisms," Proceedings of ASME 29th Mechanisms and Robotics Conference, Paper No. DETC2005-84073, pp. 3–13.
[28] Lotti, F., Zucchelli, B., Reggiani, B., and Vassura, G., 2006, "Evaluating the Flexural Stiffness of Compliant Hinges Made With Close-Wound Helical Springs," ASME 30th Annual Mechanisms and Robotics Conference.
[29] Tuijthof, G. J. M., van Engelen, S. J. M. P., Herder, J. L., Goossens, R. H. M., Snijders, C. J., and van Dijk, C. N., 2003, "Ergonomic Handle for an Arthroscopic Cutter," Min. Inv. Therapy All. Technol., **12**(1-2), pp. 82–90.